Low temperature incommensurately modulated and noncollinear spin structure in $FeCr_2S_4$

G M Kalvius[1,6], A Krimmel[2], O Hartmann[3], R Wäppling[3], F E Wagner[1], F J Litterst[4], V Tsurkan[2,5] and A Loidl[2]

[1] Physics Department, Technical University Munich, D-85747 Garching, Germany
[2] Experimental Physics V, Center for Electronic Correlations and Magnetism, Augsburg University, D-86159 Augsburg, Germany
[3] Department of Physics and Material Science, Uppsala University, S-75121 Uppsala, Sweden
[4] IPKM, Technical University Braunschweig, D-38106 Braunschweig, Germany
[5] Institute of Applied Physics, Academy of Sciences, RM-2028 Chisinau, Republic of Moldova

E-mail: kalvius@ph.tum.de

Abstract

$FeCr_2S_4$ orders magnetically at $T_N \approx 170$ K. According to neutron diffraction, the ordered state down to 4.2 K is a simple collinear ferrimagnet maintaining the cubic spinel structure. Later studies, however, claimed trigonal distortions below ~60 K coupled to the formation of a spin glass type ground state. To obtain further insight, muon spin rotation/relaxation (μSR) spectroscopy was carried out between 5 and 200 K together with new ^{57}Fe Mössbauer measurements. Below ~50 K, our data point to the formation of an incommensurately modulated noncollinear spin arrangement like a helical spin structure. Above 50 K, the spectra are compatible with collinear ferrimagnetism, albeit with a substantial spin disorder on the scale of a few lattice constants. These spin lattice distortions become very large at 150 K and the magnetic state is now better characterized as consisting of rapidly fluctuating short-range ordered spins. The Néel transition is of second order, but ill defined, extending over a range of ~10 K. The Mössbauer data around 10 K confirm the onset of orbital freezing and are also compatible with the noncollinear order of iron. The absence of a major change in the quadrupole interaction around 50 K renders the distortion of crystal symmetry to be small.

Due to unusual properties such as colossal magnetoresistance (CMR) [1, 2], multiferroicity [3–6], and strong spin–phonon coupling effects [7–10], spinels and, in particular, chromium based spinels have attracted considerable attention for many years. In the normal spinel structure AB_2X_4, the A-site ions are tetrahedrally and the B-site ions octahedrally coordinated by the X ions (oxygen, sulfur, or selenium) [11]. Both sites experience strong magnetic frustration. The A-site ions form a diamond lattice with frustration originating from competing interactions between nearest and next nearest exchange couplings [12]. The B-site ions form a pyrochlore structure, which is a geometrically frustrated three-dimensional lattice. In $FeCr_2S_4$ the magnetic couplings are transmitted by indirect exchange for both sites [11]. A variety of magnetic states between long-range order (LRO) and spin glass (SG) behavior is often formed by the action of frustration [13–16].

$FeCr_2S_4$ is a semiconductor entering LRO around 170 K. Early powder neutron diffraction data [17, 18], which compared only the 300 K and the 4.2 K patterns, reported the

[6] Author to whom any correspondence should be addressed.

LRO spin structure to be a collinear ferrimagnet formed by antiferromagnetically coupled ferromagnetic Fe and Cr sublattices. The ordered moments were derived to be $\mu_{Fe} = 4.2\ \mu_B$ and $\mu_{Cr} = 2.9\ \mu_B$. Also stated was that the cubic spinel structure is maintained at 4.2 K. In contrast, Mössbauer data of the same period indicated a structural transformation around 10 K, based on the unusual temperature dependence of the quadrupole interaction for the tetrahedrally coordinated Fe^{2+} [19, 20]. The temperature dependence of transmission electron microscopy data of single crystalline $FeCr_2S_4$ indicated a cubic to triclinic symmetry reduction at ∼60 K [21]. Previously, a cusp-like feature had been observed in the temperature dependence of the magnetization at this temperature [22], together with a separation of the field cooled and zero field cooled magnetization curves and the appearance of slow magnetic relaxation. The formation of a re-entrant SG-like state was suggested. Ultrasound measurements [23] on single crystalline $FeCr_2S_4$ found the temperature dependence of the sound velocity to be characterized by three distinct anomalies at 176, ∼60, and ∼15 K. The authors conclude that the upper value reflects the Néel temperature, the middle value the structural transition and the lower value orbital moment freezing as seen in specific heat data and dielectric spectroscopy [24].

In this communication we report on μSR spectroscopy of polycrystalline $FeCr_2S_4$, performed within a general program of μSR studies of various thio-spinels. A μSR investigation seems to be particularly appropriate for checking the stability of spin order in $FeCr_2S_4$, due to the particular sensitivity of this technique to local disorder inside long-range ordered spin lattices. In addition, we carried out Mössbauer spectroscopy on the same material with the aim of relating its hyperfine parameters to features of the μSR spectra.

A similar study on $Fe_{0.5}Cu_{0.5}Cr_2S_4$, which often serves as a model substance for understanding CMR behavior in the Cr thio-spinels, has been published recently [25]. There we showed that a spin reorientation within the ferrimagnetic spin lattice takes place around 100 K.

Polycrystalline ternary $FeCr_2S_4$ material has been prepared by solid state reaction from high-purity elements Fe (99.99%), Cr (99.99%), and S (99.999%) in evacuated quartz ampules. To prevent formation of anion vacancies known as the dominating defects in the chalcogenide spinels, the synthesis temperature was restricted to 750 °C. At this temperature the diffusion rate is rather low and, therefore, to reach complete reaction, four sintering cycles were necessary, including regrinding and pressing of the ceramics after each cycle. For each cycle the soaking time at high temperature was one week followed by slow cooling (30 °C h^{-1}) to room temperature. Annealing of the final product in sulfur atmosphere and/or vacuum was additionally performed to control the materials properties. Sample homogeneity and phase content was checked by x-ray powder diffraction at room temperature. The diffraction data indicated pure $FeCr_2S_4$ spinel and absence of spurious phases within the limit of detection (2–3%).

For the μSR measurements the powder was pressed between thin aluminized Mylar foils and positioned inside the center tube of a He-flow cryostat. The location of the sample within the He flow ensured proper, uniform, and highly stable sample temperature. The μSR spectra were measured for two separately prepared samples in zero applied field (ZF) and weak transverse field (TF) at the Swiss Muon Source (PSI) between 5 and 200 K. Surface muons in connection with either the GPS or the DOLLY spectrometers were employed. The 'veto' mode [26] was enabled which suppresses the unwanted background signal from muons stopped outside the sample. Data were taken for both samples under the same conditions at a number of temperatures. No difference in the spectra could be seen and therefore there is no need to distinguish the results according to the two sequences of measurements. The time resolution was 1.25 ns and both spectrometers have an initial dead time of 5 ns.

Details on the μSR technique can be found, for example, in [27–31]. The μSR spectrum is a plot of the measured backward–forward count rate asymmetry $A(t)$ versus time, where $t = 0$ is the time at which the muon is implanted into the sample. Usually a time span of three to four mean muon life times ($\tau_\mu = 2.2\ \mu$s) is covered. The spectrum is generally described by

$$A(t) = A_0 G(t). \tag{1}$$

Here A_0 is the initial ($t = 0$) asymmetry which depends on details of the spectrometer ($A_0 = 0.22$ in the present case). $G(t)$ is the muon spectral function reflecting the magnitude, the static distribution, and the temporal behavior of the internal magnetic field B_μ created by the magnetic moments (both atomic and nuclear) surrounding the muon at its interstitial stopping site and/or by an externally applied field. Except in metals of very high purity, one can safely assume the muon to be stationary within the temperature range covered in this study. Unfortunately, the stopping site itself is not known. Its determination usually requires single crystal data. The properties of B_μ derived from $G(t)$ can rather directly be related to the corresponding properties of the magnetic spin system. Since the atoms of the constituents (Fe, Cr, S) do not contain isotopes having nuclear dipole moments in sizable natural abundance, nuclear-electron double relaxation of muon spins [32] need not be considered.

Figure 1 shows spectra recorded at 175 and 170 K in a weak transverse field. The 175 K spectrum is typical for a paramagnet whose spectral function is

$$G(t) = \exp(-\lambda_{par} t)\cos(2\pi\nu_\mu t) \tag{2}$$

$$\text{with } \nu_\mu = \frac{\gamma_\mu}{2\pi} B_\mu, \qquad \text{and} \qquad \frac{\gamma_\mu}{2\pi} = 135.5\ \text{MHz T}^{-1}$$

being the muon gyromagnetic ratio. The relaxation rate $\lambda_{par} = \gamma_\mu^2 \langle B_\mu^2 \rangle \tau_S$ depends on the width of the distribution of B_μ characterized by its second moment (static relaxation) and the spin fluctuation rate $1/\tau_S$ (dynamic relaxation). B_μ is essentially the applied transverse field, except for a small change caused by the magnetization of the paramagnet in an external field (muon Knight shift). This is negligible here on account of the low applied field (TF = 3 mT). At 170 K the spectrum consists of two sub-spectra. The oscillatory pattern having intensity A_p is the μSR response of a paramagnetic

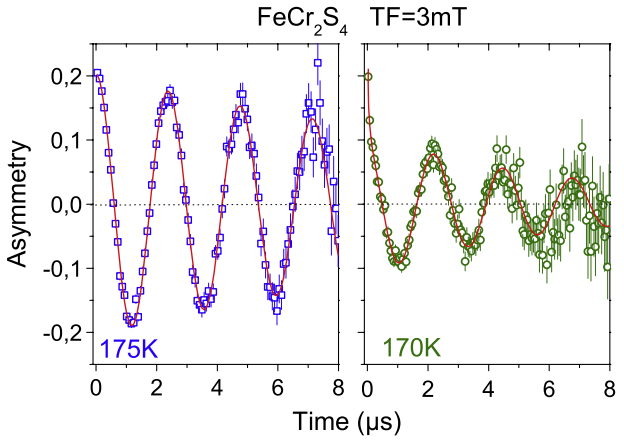

Figure 1. TF = 3 mT spectra of $FeCr_2S_4$ above and near the magnetic ordering temperature. The solid lines are least squares fits to a single oscillatory signal (equation (2)) at 175 K with $\chi^2 = 1.12$ and to two signals (one oscillatory, the other a rapid exponential relaxation relevant at early times) at 170 K with $\chi^2 = 1.06$. The origin of these different spectral functions is discussed in the text.

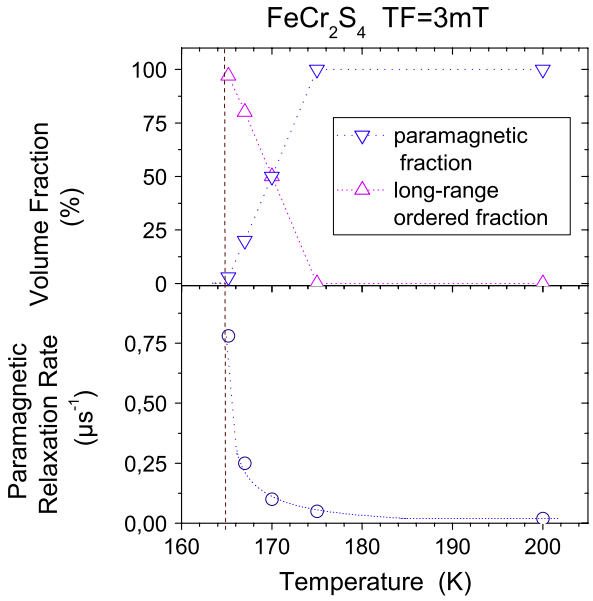

Figure 2. Temperature dependences of the volume fractions of the paramagnetic and the LRO states (top), and of the paramagnetic relaxation rate (bottom). The lines are guides to the eye.

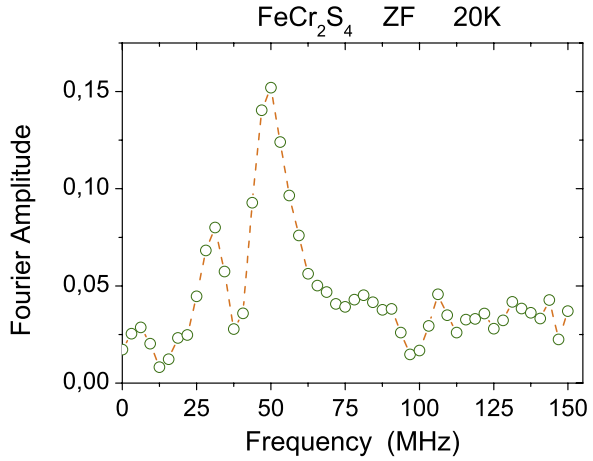

Figure 3. Fast Fourier transform of the ZF spectrum of $FeCr_2S_4$ at 20 K. The line is a guide to the eye only.

fraction. The second signal, having intensity A_m shows a rapidly relaxing asymmetry and is considered to reflect a magnetically ordered fraction. The condition $A_p + A_m = A_0$ must be fulfilled and the relative intensities A_p/A_0 and A_m/A_0 are directly the volume fractions of two coexisting magnetic states. Figure 2 displays the temperature dependences of the parameters of the TF spectra between 200 and 165 K. It is seen that at around 175 K the formation of an ordered fraction sets in. At 165 K nearly all of the sample volume has entered the ordered state. Clearly, the transition between the ordered and the paramagnetic phases is broadened, extending over ∼10 K. The broad transition range easily explains the scatter of T_N around 170 K reported in the literature. The relaxation rate λ_{par} rises sharply on approach to T_N from above, reflecting critical slowing down of the paramagnetic spins (i.e. increase of τ_S). This behavior indicates the Néel point to be a second-order phase transition.

As mentioned, the magnetically ordered state below T_N is usually considered to be a simple collinear ferrimagnetic spin structure. In that case the ZF spectral function for a polycrystalline powder sample is

$$G(t) = \tfrac{2}{3}\exp(-\lambda_{trans}t)\cos(2\pi\nu_\mu t) + \tfrac{1}{3}\exp(-\lambda_{long}t). \quad (3)$$

The two terms (transverse and longitudinal) arise from the usual approach to describe the isotropic average by assuming that two thirds of the muons see an internal field perpendicular to the initial orientation of their spins, resulting in a muon spin precession. For the remaining third of the muons, the internal field is oriented parallel to the muon spins and no precession takes place. However, dynamic muon spin depolarization, caused by the fluctuations of the magnetic moments surrounding the muon, is described by the longitudinal term. The longitudinal relaxation rate λ_{long} is directly proportional to the magnetic spin fluctuation rate $1/\tau_S$. In the transverse term, muon spin relaxation is visible as damping of the oscillatory pattern. The damping rate λ_{trans} originates from the static distribution of B_μ and the fluctuations of the magnetic moments. In general $\lambda_{long} \ll \lambda_{trans}$, which allows us to neglect the dynamic contribution in the first term. Then λ_{trans} can be seen as a direct measure of the width of the distribution of B_μ coming from local disorder in the LRO spin array.

Turning now to the low temperature data, one notices that even a cursory inspection of the ZF spectra (e.g. at 20 K) shows that they are more complex in appearance than described by equation (3). Fast Fourier transforms (FFTs) of these spectra clearly show the presence of two oscillatory frequencies. An example is displayed in figure 3, where an upper frequency (UFR) of $\nu_U \approx 50$ MHz, and a lower frequency (LFR) of $\nu_L \approx 30$ MHz can be discerned. The spectrum needs to be analyzed using the sum of two signals given by equation (3) with relative intensities A_U/A_0 and A_L/A_0, respectively. One

Table 1. Parameters of the μSR spectrum of $FeCr_2S_4$ at 20 K. These numbers are typical for all spectra in the regime $T \leqslant 40$ K.

A_U (%)	ν_U (MHz)	$\lambda_{\mathrm{trans},U}$ (μs^{-1})	A_L (%)	ν_L (MHz)	$\lambda_{\mathrm{trans},L}$ (μs^{-1})	λ_{long} (μs^{-1})
71	49.3	8	29	30.8	20	0.025

can simplify the situation somewhat by assuming that both signals have the same longitudinal rate λ_{long}. There is one additional problem to be taken care of. Due to the rapid initial decay of $A(t)$ on account of the relatively high frequencies, one loses the very early part of the spectrum in the initial dead time of the spectrometer. This means that data points close to $t = 0$ are not visible and hence A_0 cannot be obtained directly. The total signal intensity of μSR spectra measured under identical geometric conditions must be independent of temperature. This allows us to fix the initial amplitude to $A_0 = 0.22$ obtained from the TF spectra at high temperatures (see figure 1).

Unfortunately, a least squares fit based on the considerations just outlined remained unsatisfactory. The cause is the large difference in amplitude between the first (at $t = 0$) and the second (at $t = 1/\nu$) maximum of the oscillatory pattern, while the following maxima are much less reduced in their amplitudes (see, for example, figure 4, top). Such a feature cannot be described via exponential (or for that matter Gaussian) damping when insisting on $A_0 = 0.22$. A strong reduction between the first two oscillatory amplitudes is, however, a feature of Bessel oscillations, meaning one has to replace equation (3) by

$$G(t) = \tfrac{2}{3}\exp(-\lambda_{\mathrm{trans}}t)J_0(2\pi\nu_\mu t) + \tfrac{1}{3}\exp(-\lambda_{\mathrm{long}}t) \qquad (4)$$

where J_0 is the zero order Bessel function. Least squares fits to the low temperature spectra using the sum of two Bessel patterns, again with identical longitudinal terms, were quite successful with values of the goodness of fit parameter χ^2 between 1.0 and 1.1. A pertinent example is shown in figure 4, upper panel. Although the plot only shows the early times, the least squares fit extended over the full range measured 0–9 μs. The spectral parameters of the 20 K data are listed in table 1. Frequencies and relative intensities correspond well to the Fourier plot. The low value of the longitudinal relaxation rate means that the spin system is essentially static. Also, remarkable are the moderate values of the transverse relaxation rates, indicating fairly well developed long-range order. Bessel oscillations in a μSR spectrum appear in cases of incommensurately modulated spin structures [33, 34]. Such a spin array then characterizes the magnetic ground state of $FeCr_2S_4$. We return to a more detailed discussion of this result further below after having looked at the μSR spectra at more elevated temperatures within the LRO regime.

At 40 K a sudden strong increase of λ_{trans} occurs in the spectral patterns, making the oscillatory features in the spectra barely visible. A characteristic spectrum is shown in figure 4, the lower panel. The Fourier transform also shows only a broad, poorly developed peak with no structure. A fit with

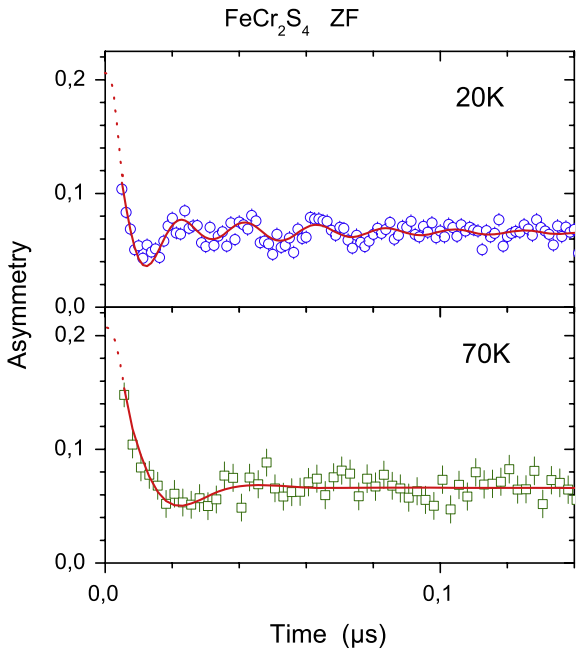

Figure 4. Early part of the ZF spectra of $FeCr_2S_4$ at 20 K (top) and 70 K (bottom). The solid lines are the least squares fit discussed in the text giving $\chi^2 = 1.04$ at 20 K and 1.05 at 70 K. The broken lines are the extensions of the fits into the spectrometer dead time region.

two frequencies no longer makes sense. In fact, if enforced, it damps out the UFR pattern immediately. Furthermore, there is no difference in fit quality whether one uses cosine or Bessel oscillation. Therefore, all spectra for 40 K $\leqslant T < T_{\mathrm{N}}$ were analyzed using equation (3) with fixed $A_0 = 0.22$.

The temperature dependences of the spectral parameters of $FeCr_2S_4$ obtained as described for $T < T_{\mathrm{N}}$ are plotted in figure 5. There is little variation of parameters within the regime where two frequencies are present. A slight rise in A_L can be discerned when increasing the temperature from 2 to 15 K, but it is barely outside the error. Above 150 K the transverse relaxation rises significantly once more. The initial decay of $A(t)$ is now given by λ_{trans} rather than the first oscillatory peak, which makes the determination of ν_μ difficult and its values uncertain. The drop of ν_μ on the final approach to T_{N} cannot be substantiated, but is consistent with the behavior of λ_{par} above T_{N} indicating, as pointed out, a second-order phase transition. According to the temperature variation of the longitudinal relaxation, the system of magnetic spins leaves the nearly static limit above 100 K reaching a fairly high spin fluctuation rate close to T_{N}.

We now turn to the discussion of the information to be drawn from the μSR spectra of $FeCr_2S_4$. Data taken well within the paramagnetic regime ($T \geqslant 175$ K) are clear indications that only one single crystallographic muon stopping site exists, although its location is unknown. The existence of a unique muon stopping site is also verified by the μSR spectra of $Fe_{0.5}Cu_{0.5}Cr_2S_4$ [25]. Hence, the two signal μSR response at $T < 40$ K in $FeCr_2S_4$ must intimately be connected to a change in magnetic structure. This leads directly to the main conclusion that $FeCr_2S_4$ does not possess a simple collinear ferrimagnetic ground state as originally

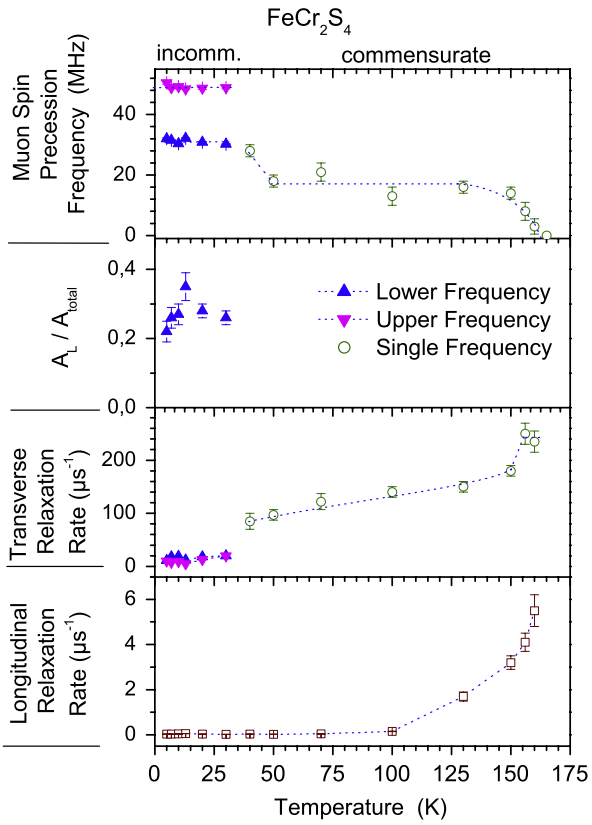

Figure 5. Temperature dependences of the spectral parameters of $FeCr_2S_4$ in the magnetically ordered regime obtained from the least squares fits discussed in the text. The dotted lines are guides to the eye.

suggested [17, 18]. If that was the case, one would observe a moderately damped single frequency sinusoidal oscillatory pattern, as was the case in the low temperature spectra of $Fe_{0.5}Cu_{0.5}Cr_2S_4$, where the simple collinear ferrimagnetic ground state is well established. Similarly, we can exclude the suggested [22] SG magnetic ground state. The μSR spectral pattern for an SG is unique (Kubo–Toyabe relaxation) [35] which is in the present case altogether incompatible with the observed low temperature spectra.

According to the presence of Bessel oscillation, $FeCr_2S_4$ must have an incommensurately modulated spin structure as its magnetic ground state. Basically two types of spin modulations exist. Either the moment magnitude, or the moment orientation is modulated. The pertinent example of the first case is the spin density wave (SDW) where the moment magnitude is sinusoidally modulated [36]. The simplest realization of the second case is a helical spin arrangement [37]. The internal field B_μ is generated predominantly, at least in poor conductors, by the anisotropic dipole field of the moments surrounding the muon. Hence it is sensitive to the magnitude and the orientation of these moments. In contrast, $B_{\rm hf}$ measured by Mössbauer spectroscopy is isotropic and sensitive only to the magnitude of the moment on the resonant atom. The classical case of a sinusoidally modulated incommensurate spin structure studied by Mössbauer spectroscopy is Tm metal [38, 39] for 56 K $> T >$ 40 K. The ^{169}Tm spectra show, as expected, a wide distribution in $B_{\rm hf}$. Characteristic is the presence of small fields which results in enhanced intensity at the center of the spectrum. In the case of $FeCr_2S_4$ the published Mössbauer spectra at low temperatures [20] show a well defined $B_{\rm hf}$ and no additional intensity at the center. Our own Mössbauer data, which will be discussed in more detail further below, gave basically the same result. Therefore a modulation of moment magnitude must be excluded, leading to the conclusion that $FeCr_2S_4$ forms an incommensurate helical spin array below 40 K. The distribution of internal field magnitude seen by μSR for such a spin structure has an 'M'-shape [40]. It peaks at a minimum field $B_\mu^{\rm min}$ which is different from zero, goes through a valley and peaks again at the maximum field $B_\mu^{\rm max}$. The peak at $B_\mu^{\rm min}$ is lower than that at $B_\mu^{\rm max}$. The distribution of B_μ (or ν_μ) revealed in the Fourier plot of the spectrum taken at 20 K (figure 3) corresponds well to the field distribution described in [40]. Thus the appearance of two frequencies, corresponding to $B_\mu^{\rm min}$ and $B_\mu^{\rm max}$, respectively, is a natural outcome for an incommensurate spin helix.

Since μSR is a real space technique, it is unable to reveal the exact spin arrangement. It is probably quite complex since we have to consider two spin sub-lattices. Two antiferromagnetically coupled cone-like spiral structures are a distinct possibility. Strictly speaking, the exclusion of moment magnitude modulation only holds for the Fe sub-lattice. If the muon site was known, one could model possible spin structures and calculate the resulting field distribution to be compared with the μSR data.

To summarize, the conclusion in favor of the presence of some cone-like helical structure is based on the combination of the present μSR data and known Mössbauer and bulk magnetic data. The Bessel-type μSR signal indicates an incommensurately modulated spin system. The Mössbauer spectra exclude moment magnitude modulation, meaning that orientational modulation of the moments (helical spin structure) is present. The observation of a two frequency μSR signal (from a single muon stopping site) is compatible with a spin helix. Bulk magnetic data have established a ferrimagnetic ground state. This then requires a cone-like spin arrangement to produce ferromagnetic components. The exact geometrical nature of this helical state cannot be inferred from the present data. As it stands now, precise neutron diffraction measurements are urgently called for.

At 40 K the transverse relaxation rate increases suddenly and sharply. It reflects substantial spin disorder on a local scale in the magnetic structure above 40 K. In $Fe_{0.5}Cu_{0.5}Cr_2S_4$ such an increase of $\lambda_{\rm trans}$ occurred as well (around 90 K), but the damping decreased on further raising the temperature. This is not the case in $FeCr_2S_4$ where $\lambda_{\rm trans}$ stays high and even increases further on warming. Also in $Fe_{0.5}Cu_{0.5}Cr_2S_4$ the spectral type did not fundamentally change above 90 K while in $FeCr_2S_4$ at 40 K a switch from a two frequency to a single frequency spectrum together with a likely change from incommensurability to commensurability takes place. This is then not a mere spin reorientation transition. The data rather indicate the development between 40 and 50 K of a new LRO state whose μSR spectra are compatible with a simple collinear

ferrimagnetic spin structure having strong local disturbances. This spin disorder is substantially larger in $FeCr_2S_4$ compared to $Fe_{0.5}Cu_{0.5}Cr_2S_4$. Whether the change in spin structure around 40 K is connected to the triclinic distortion reported to occur at 60 K [21] cannot be decided by μSR. The difference in characteristic temperatures may again arise from differences between single crystalline and powder samples. The final approach to T_N sees another major increase of λ_{trans} in $FeCr_2S_4$. This feature is also not present in $Fe_{0.5}Cu_{0.5}Cr_2S_4$ where λ_{trans} saturates at a comparatively low value near T_N. One may question whether one can still speak of an LRO spin arrangement above ~150 K in $FeCr_2S_4$ since the width of the field distribution ($\Delta B_\mu \approx 250$ mT) is much larger than the mean field ($\langle B_\mu \rangle \approx 50$ mT). The actual situation may be a nearly random, dynamically short-range ordered spin state.

Over the whole helical state, the spin system remains essentially static ($\lambda_{long} \approx 0$). In the collinear ferrimagnetic state the temperature dependence of λ_{long} is quite similar to that seen in $Fe_{0.5}Cu_{0.5}Cr_2S_4$, that is, a monotonic rise on approach to T_N. A possible explanation of this feature is given in [25] based on theoretical considerations outlined in [41]. Neither in $Fe_{0.5}Cu_{0.5}Cr_2S_4$ nor in $FeCr_2S_4$ does one observe any irregularity in λ_{long} at the transition points of 90 or 40 K, respectively.

The Néel transition is of second order and not well defined. The paramagnetic fraction rises continuously between 165 and 175 K. Above 175 K the whole sample is in a weakly correlated, paramagnetic spin state. It does not split into two fractions, one weakly, the other strongly spin correlated as has been observed, for example, in the frustrated spinel system MAl_2O_4 with M, = Mn, Fe, Co [16].

Finally, we briefly discuss the Mössbauer data. Of the several studies available [19, 20, 42, 43] none presents data over the whole temperature range of interest (4.2 to ~200 K). For this reason, and in order to have data on the same material used in the μSR work, we have carried out a new Mössbauer study. Overall, our spectra have the same form as those shown in previous studies.

The iron is, as expected, in the divalent charge state. A small fraction of iron atoms (<5%) is in the 3+state. They are visible in spectra with very good statistical accuracy by the outermost resonance lines of a magnetic hyperfine pattern, but the inner resonance lines cannot be resolved from the dominating Fe^{2+} signal and thus we have no information on the chemical nature of the trivalent iron. The visible part of the Fe^{3+} resonance remains essentially unaltered between 4 and ~100 K, a temperature region where the Fe^{2+} resonance changes markedly. At higher temperature the Fe^{3+} signal can no longer be seen because the magnetic hyperfine splitting has collapsed. The decoupling between the 2+ and 3+ signals points strongly towards the presence of an impurity phase whose fraction is below the sensitivity of the original x-ray diffraction (XRD) check. It is also not unlikely that the Fe^{3+} ions were created in the additional fine powdering of the material needed to produce a uniform Mössbauer absorber. This increases the sensitive surface area and it has recently been observed in an x-ray photo-electron and absorption study of $Fe_{1-x}Cu_xCr_2S_4$ that Fe^{3+} ions were present at surfaces

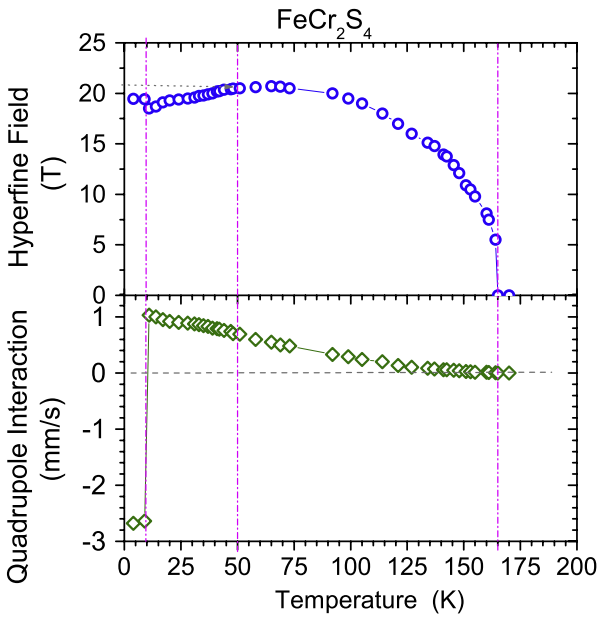

Figure 6. ^{57}Fe Mössbauer data of $FeCr_2S_4$: Temperature dependences of the hyperfine field B_{hf} (top) and the quadrupole interaction QI (bottom). The solid lines are guides to the eye. The dash-dotted lines mark the temperature at which irregularities occur. The dotted line is the extrapolation of B_{hf} if no change at 50 K occurred.

which had been absent in the sample as-grown [44]. As stated earlier, the strength of a μSR signal is directly proportional to the volume fraction of the corresponding compound. For a fraction in the few per cent region the signal will be hidden in the statistical fluctuations of the main signal and hence the conclusion drawn from the μSR spectra of $FeCr_2S_4$ remains unaffected.

The Mössbauer spectra in the paramagnetic regime show the expected unbroadened single resonance line. Together with the appearance of a magnetic hyperfine field B_{hf} below 165 K an electric quadrupole interaction (QI) also appears. Its magnitude rises continuously on cooling to 10 K (see figure 6). The existence of a QI is unexpected because of the cubic (tetrahedral) coordination of Fe on the spinel A-site. The electric field gradient (EFG) present for $T < T_N$ is probably generated by the mechanism known as 'magnetically induced quadrupole interaction', a consequence of spin–orbit coupling. Such a behavior is commonly observed in f-element materials and easily treated theoretically [45]. In transition element compounds the effect is usually small and its theoretical treatment is considerably more complex. The case of Fe^{2+} in a cubic environment is dealt with extensively in [46]. The main point is that the induced EFG is essentially oriented parallel to B_{hf}. Our Mössbauer spectra above 50 K reveal small axial EFGs with a slight distribution which may originate from the presence of small Euler angles between field gradient axes and the magnetic hyperfine field. The reason could be a minor lattice distortion leaving the collinear magnetic arrangement undisturbed. No major change in QI is seen at 50 K where a change in crystal symmetry has been reported. An additional lattice EFG is possible, but it must be rather small. The

distortion of the spinel lattice is minute. It should be kept in mind, however, that the detection of the lattice distortion [21] was performed with a single crystal and that the method used (electron diffraction) senses the surface of the specimen. It could be a surface reconstruction and not a bulk effect.

According to the μSR spectra, the transition into the helical spin array occurs between 50 and 40 K. The major part of the EFG remains magnetically induced and the EFG is therefore locked in the direction of $B_{\rm hf}$. The presence of a well defined EFG is thus no contradiction to an orientationally modulated magnetic structure. A dramatic alteration of the QI, affecting both magnitude and sign, occurs around 10 K. This has been seen before [20]. In view of the results reported in [24], one can attribute this feature to the onset of orbital ordering. The d-orbits are now spatially fixed, which clearly affects the QI profoundly. A careful analysis of line positions and intensities of the Mössbauer spectra using a Hamiltonian including EFG and magnetic hyperfine interaction with the proper Euler angles [47], reveals that in this temperature range we have iron sites with identical EFGs yet different angles between the EFG main axes and the magnetic field. This clearly speaks for a spiral or helical spin structure, in agreement with the conclusions drawn from μSR. The μSR parameters are not significantly affected around 10 K (see figure 5), meaning that the ordered moments do not change. A detailed discussion of the Mössbauer data taking into account the electronic level structure in crystalline electric field of iron for the present case is forthcoming [47].

In the temperature dependence of $B_{\rm hf}$ a somewhat unusual behavior occurs around 165 K. At 163 K the spectrum clearly shows magnetic hyperfine splitting, but at 165 K no hyperfine splitting is present. In contrast, the μSR spectrum is still magnetic at 165 K which is the lower border temperature where a paramagnetic fraction appears (see figure 2). Only above 175 K does μSR see a fully paramagnetic compound. Obviously the responses of Mössbauer and μSR spectroscopies in the transition region to paramagnetism are different. This might be connected to the presence of the highly dynamic short-range ordered state formed according to μSR above 150 K. The two methods sense spin fluctuations differently and it appears that, on the timescale of ^{57}Fe hyperfine interactions, this spin state is viewed as a paramagnetic state. Between 150 and 50 K the temperature dependence of $B_{\rm hf}$ is a monotonous rise, but beginning around 50 K the field decreases on cooling rather than rising slightly toward saturation. The result suggests that the spin structure above and below $\sim$50 K is not the same, as verified by μSR, but the smallness of the change in $B_{\rm hf}$ shows that a major change in electronic structure does not take place. The slight irregularity in $B_{\rm hf}(T)$ around 10 K cannot be guaranteed. The number of parameters has increased (e.g. Euler angle and asymmetry parameter) which makes it difficult to find the correct best fit. The main finding, namely the dramatic change in QI is independent of the fit procedure.

In conclusion, the main result of this study is that the notion of a simple collinear ferrimagnetic structure over the whole temperature range below $T_{\rm N}$ is not correct. The magnetic ground state of $FeCr_2S_4$ is based on helical spin structures appearing below $\sim$50 K. This is important due to the fact that $FeCr_2S_4$ could be a further candidate for spin-driven ferroelectricity [48]. In these compounds, spiral spin order can break inversion symmetry and spontaneous polarization is induced via an inverse Dzyaloshinskii–Moriya interaction. So far there is no proof for ferroelectricity in the title compound and dielectric studies cannot easily be interpreted due to enhanced conductivity contributions. Detailed experiments are, however, in progress to investigate this issue.

The pronounced change in quadrupole interaction seen in the Mössbauer spectra verifies the occurrence of orbital ordering around 10 K. Neither $B_{\rm hf}$ of ^{57}Fe nor B_μ are seriously affected at this temperature, indicating that no change in moment magnitude occurs.

Above $\sim$50 K, the μSR data are consistent with the normal ferrimagnetic structure commonly ascribed to $FeCr_2S_4$ which, however, possesses in addition marked local disorder (over the distance of a few lattice constants) in its LRO spin arrangement. This disorder, accompanied by a rising fluctuation rate, becomes so pronounced above 150 K that up to $T_{\rm N} = 170 \pm 5$ K, as defined by μSR and susceptibility, the spin state is better described as consisting of rapidly fluctuating short-range ordered spins. The transition into paramagnetism as seen by μSR is of second order but exhibits a roughly 10 K spread. It is noticed that the spectral response to the dynamic short-range ordered state is different for μSR and Mössbauer spectroscopy.

This work was supported by the Deutsche Forschungsgemeinschaft (DFG) via SFB484/Augsburg. The μSR studies were performed at the Swiss Muon Source, Paul Scherrer Institute (PSI), Villigen, Switzerland. We thank R Scheuermann, H Luetkens, and A Amato for their help in carrying out the experiments.

References

[1] Ramirez A P, Cava R J and Krajewski J 1997 *Nature* **386** 156
[2] Fritsch V, Deisenhofer J, Fichtl R, Hemberger J, Krug von Nidda H-A, Mücksch M, Nicklas M, Samusi D, Thompson J D, Tidecks R, Tsurkan V and Loidl A 2003 *Phys. Rev.* B **67** 144419
[3] Siratori K and Kita E 1980 *J. Phys. Soc. Japan* **48** 1443
[4] Hemberger J, Lunkenheimer P, Fichtl R, Krug von Nidda H-A, Tsurkan V and Loidl A 2005 *Nature* **434** 364
[5] Yamasaki Y, Miyasaka S, Kaneko Y, He J-P, Arima T and Tokura Y 2006 *Phys. Rev. Lett.* **96** 207204
[6] Weber S, Lunkenheimer P, Fichtl R, Hemberger J, Tsurkan V and Loidl A 2006 *Phys. Rev. Lett.* **96** 157202
[7] Sushkov A B, Tchernyshyov O, Ratcliff W, Cheong S W and Drew H D 2005 *Phys. Rev. Lett.* **94** 137202
[8] Hemberger J, Rudolf T, Krug von Nidda H-A, Mayr F, Pimenov A, Tsurkan V and Loidl A 2006 *Phys. Rev. Lett.* **97** 087204
[9] Hemberger J, Krug von Nidda H-A, Tsurkan V and Loidl A 2007 *Phys. Rev. Lett.* **98** 147203
[10] Rudolf T, Kant Ch, Mayr F, Hemberger J, Tsurkan V and Loidl A 2007 *New J. Phys.* **9** 76
[11] van Stapele R P 1982 *Ferromagnetic Materials* vol 3, ed E P Wohlfarth (Amsterdam: North Holland) p 606
[12] Bergman D, Alicea J, Gull E, Trebst S and Balents L 2007 *Nat. Phys.* **3** 487

[13] Fritsch V, Hemberger J, Büttgen N, Scheidt E-W, Krug von Nidda H-A, Loidl A and Tsurkan V 2004 *Phys. Rev. Lett.* **92** 116401
[14] Krimmel A, Mücksch M, Tsurkan V, Koza M M, Mutka H and Loidl A 2005 *Phys. Rev. Lett.* **94** 237402
[15] Krimmel A, Mücksch M, Tsurkan V, Koza M M, Mutka H, Ritter C, Sheptyakov D V, Horn S and Loidl A 2006 *Phys. Rev.* B **73** 014413
[16] Kalvius G M, Krimmel A, Hartmann O, Litterst F J, Wagner F E, Tsurkan V and Loidl A 2010 in preparation
[17] Shirane G, Cox D E and Pickard S J 1964 *J. Appl. Phys.* **35** 954
[18] Broquetas Colominas C, Ballestracci R and Roult G 1964 *J. Physique* **25** 526
[19] Eibschutz M, Shtrikman S and Tennebaum V 1967 *Phys. Lett.* A **24** 563
[20] Spender M R and Morrish A H 1972 *Solid State Commun.* **11** 1417
[21] Mertinat M, Tsurkan V, Samusi D, Tidecks R and Haider F 2005 *Phys. Rev.* B **71** 100408
[22] Tsurkan V, Baran M, Szymczak R, Szymczak H and Tidecks R 2001 *Physica* B **296** 301
[23] Maurer D, Tsurkan V, Horn S and Tidecks R 2003 *J. Appl. Phys.* **93** 9173
[24] Fichtl R, Fritsch V, Krug von Nidda H-A, Scheidt E-W, Tsurkan V, Lunkenheimer P, Hemberger J and Loidl A 2005 *Phys. Rev. Lett.* **94** 027601
[25] Kalvius G M, Hartmann O, Krimmel A, Wagner F E, Wäppling R, Tsurkan V, Krug von Nidda H-A and Loidl A 2008 *J. Phys.: Condens. Matter* **20** 252204
[26] Arsenau D J, Hitti B, Kreitzmann S R and Whidden E 1997 *Hyperfine Interact.* **106** 277
[27] Kalvius G M, Noakes D R and Hartmann O 2001 *Handbook on the Physics and Chemistry of Rare Earth* vol 32, ed K A Gschneidner *et al* (Amsterdam: Elsevier Science) p 55ff
[28] Lee S L, Kilcoyne S H and Cywinski R (ed) 1999 *Muon Science* (London: Institute of Physics Publishing)
[29] Davis E A and Cox S F 1996 *Protons and Muons in Material Science* (London: Taylor and Francis)
[30] Karlsson E 1995 *Solid State Phenomena as seen by Muons, Protons and Excited Nuclei* (Oxford: Oxford University Press)
[31] Schenck A 1985 *Muon Spin Rotation Spectroscopy* (Bristol: Adam Hilger)
[32] Noakes D R, Brewer J H, Harshman D R, Ansaldo E J and Huang C Y 1987 *Phys. Rev.* B **35** 6597
[33] Le L P, Heffner H, Thompson J D, MacLaughlin D E, Nieuwenhuis G J, Amato A, Feyerherm R, Gygax F N, Schenck A, Canfield P and Cho B K 1996 *Phys. Rev.* B **53** R510
[34] Amato A 1997 *Rev. Mod. Phys.* **69** 1119
[35] Uemura Y J 1999 *Muon Science* ed S L Lee, S H Kilcoyne and R Cywinski (London: Institute of Physics Publishing) p 85ff
[36] Overhauser A W 1960 *J. Phys. Chem. Solids* **13** 71
[37] Jensen J and Mackintosh A R 1991 *Rare Earth Magnetism* (Oxford: Clarendon)
[38] Kalvius M, Kienle P, Eicher H, Wiedemann W and Schüler C 1963 *Z. Phys.* **172** 231
[39] Cohen R L 1968 *Phys. Rev.* **169** 432
[40] Noakes D R 2002 *An Ornamental Garden of Field Distributions and Static ZF Muon Spin Relaxation Functions* http://musr.org/intro/ppt/GardenExport
[41] Dalmas de Réotier P, Gubbens P C M and Yaouanc A 2004 *J. Phys.: Condens. Matter* **16** S4687
[42] Hoy G R and Singh K P 1968 *Phys. Rev.* **172** 514
[43] Klencsár Z, Kuzmann E, Homonnay Z, Vértes A, Simopoulos A, Devlin E and Kallias G 2003 *J. Phys. Chem. Solids* **64** 325
[44] Taubitz C, Kuepper K, Raekers M, Galakhov V R, Felea V, Tsurkan V and Neumann M 2009 *Phys. Status Solidi* b **246** 1470
[45] Ofer S, Nowik I and Cohen S G 1968 *Chemical Apllications of Mössbauer Spectroscopy* ed V I Goldanskii and R H Herber (New York: Academic) p 441
[46] Ganiel U and Shtrikman S 1968 *Phys. Rev.* **167** 258
[47] Wagner F E, Litterst F J, Kalvius G M, Krimmel A, Tsurkan V and Loidl A 2010 in preparation
[48] Cheong S-W and Mostovoy M 2007 *Nat. Mater.* **6** 13